Cellular and Molecular Bioengineering, Vol. 1, No. 1, March 2008 *(© 2008)* pp. 67–74
DOI: 10.1007/s12195-008-0002-1

Membrane Deformability and Membrane Tension of Single Isolated Mitochondria

SHIQI WANG,[1] CHUNSUN JIANG,[2] YAN ZHANG,[1] JUAN CHEN,[1] BIN WANG,[2] QUAN CHEN,[2] and MIAN LONG[1]

[1]National Microgravity Laboratory, Center for Biomechanics and Bioengineering, Institute of Mechanics, Chinese Academy of Sciences, Beijing 100190, P.R. China; and [2]The Laboratory of Apoptosis and Cancer Biology, The National Key Laboratory of Biomembrane and Membrane Biotechnology, Chinese Academy of Sciences, Beijing 100101, P.R. China

(Received 7 December 2007; accepted 23 January 2008; published online 4 March 2008)

Abstract—Mitochondria dynamics is crucial to many biological processes such as mitochondria fusion and fission, which is highly correlated to the mechanics of single mitochondria. However, the mechanobiological coupling of mitochondria has been poorly understood. Here membrane deformability and membrane tension of individual mitochondria isolated from MtDsRed labeled human embryonic T-Rex-293 kidney cells were measured using a micropipette aspiration assay. The results demonstrated that membrane deformation of isolated mitochondria exhibited an elastic transition phase followed by an equilibrium phase, and mitochondrial membrane tension was proportional to the area compressibility. It was also indicated that mitochondrial membrane deformability was significantly affected by physical–chemical factors such as osmotic pressure or pH value, and was further correlated to mitochondrial functionality in different respiratory states and Ca^{2+} regulation. These findings provide a new insight into understanding the mechanical regulation of mitochondrial physiology.

Keywords—Mechanical properties, Physical–chemical environment, Respiratory state, Membrane permeability transition.

INTRODUCTION

Mitochondria play a central role in determining cell life and death. Mitochondrial deficiencies accumulating with time are crucial to many pathophysiological processes such as Parkinson's disease, Alzheimer's disease, diabetes mellitus, liver disease, muscle dystrophy, cardiomyopathy, and cancer.[3,7,10] As an important subcellular compartment in almost all kinds of eukaryotic cells, mitochondria have the structure that contains the outer membrane, the intermembrane space, the inner membrane, and the matrix. The inner membrane is highly folded into cristae, in which there are the complexes of electron transport chain and ATP synthase that control the basic rates of cellular metabolism. In the past decade, mitochondria are mostly considered to serve as fundamental elements in biochemical signaling since current approaches have enabled to examine dynamic functionality and behavior of mitochondria.[18]

To perform their biological functions in electron transfer and respirations, mitochondria are required to form a highly dynamic, continuously-evolved reticulum or network in a cell, not only for the evolution of morphology but also for the manipulation of size distribution and copy number. For example, mitochondria in differentiated cells are often localized to specific cytoplasmic regions rather than randomly distributed.[24] Mitochondria also proceed a continuous cycle of dynamic fusion and fission in a live cell. During the cycle, mitochondria undergo retrograde and anterograde movements along the microtubule in combination with such motor proteins as myosins, dyneins, or kinesins.[9,21,22] Mitochondrial movement, fusion and fission are often accompanied with their own active deformation, suggesting that mechanics of mitochondria play an important role in the process. In a reconstructed vesicle of cardiolipin which is the unique negatively charged lipid appearing predominantly within the inner mitochondrial membrane, both apparent area compressibility modulus and lysis tension are found to decrease with increasing cardiolipin content.[15] To date, however, mechanics of mitochondria and their relevance to biological functionalities have not been well understood.

In the present work, a quantitative *in vitro* approach was developed to investigate mechanics of isolated mitochondria and their correlation with mitochondrial functionality in respiration. Individual mitochondria

Address correspondence to Mian Long, National Microgravity Laboratory, Center for Biomechanics and Bioengineering, Institute of Mechanics, Chinese Academy of Sciences, Beijing 100190, P.R. China. Electronic mail: mlong@imech.ac.cn

were isolated from human embryonic T-Rex-293 kidney cell lines labeled with MtDsRed. Membrane deformability and membrane tension, which are important constituent of mitochondrial membrane mechanics, were then measured using a micropipette aspiration assay, a well-developed technique widely used in cell mechanics and rheology.[8,14,23] Our results indicated that membrane deformation of isolated mitochondria exhibited an elastic transition phase followed by a saturation phase, and their respiratory functionality was coupled to the membrane tension of mitochondria.

MATERIALS AND METHODS

Reagents

CCCP (carbonyl cyanide 3-chlorophenylhydrazone) and antimycin were purchased from Sigma Chemical Co. (London, UK). CsA (cyclosporine A) was purchased from Calbiochem (San Diego, USA). All other reagents were from Beijing Chemical Reagents Company (Beijing, China) with the highest purity commercially available.

Cell Transfection, Culture and Mitochondria Isolation

Human embryonic T-Rex-293 kidney cells (Invitrogen, USA) were transfected by MtDsRed, a plasmid encoding a mitochondrial matrix-targeting protein, using DMRIE-c (Life Science, USA) upon the manufacturer's instructions. Transfected cells were grown up in Dulbecco's modified Eagle medium (DMEM) (Hyclone, Logan, USA) containing 10% heat-inactivated fetal bovine serum (FBS) (Gibco, Tulsa, USA) and 1% of penicillin and streptomycin each (Hyclone, Logan, USA). For mitochondria isolation, cells were harvested by 0.25% trypsin (Hyclone, Logan, USA). The suspension were centrifuged at 1500 rpm for 3 min and washed in PBS (Ca^{2+}- and Mg^{2+}-free). Cell pellets were then resuspended in 150 μL of Dounce buffer (210 mM sucrose/70 mM mannitol/1 mM EGTA/10 mM HEPES, pH 7.4) on ice for 30 min, and the cell suspension was transferred to the Dounce homogenizer embedded on ice. Homogenization was accomplished by 30–40 vigorous, directly vertical passes of muller B. Resulted homogenate was transferred to an eppendorf tube and the supernatant was collected after being centrifuged at 800 *g* for 10 min. Again, the collected supernatant was re-centrifuged at 10,000 *g* for 10 min and the final precipitate (mostly mitochondria) was resuspended in 50 μL Dounce buffer on ice.

Electron Microscopy Observation

Isolated mitochondria as above were fixed with 2.5% glutaraldehyde for 15 min. After fixation, the samples were washed thoroughly with PBS and fixed in 1% Os_2O_4 for 2 h at 4 °C. Dehydrated samples were embedded in Spur^{TM} for 24 h at 65 °C. After being stained with uranyl acetate and lead citrate, the sections were observed using a transmission electron microscope (TEM) (Tecnai 20, Fei, Hillsboro, USA), and the images were collected by a CCD Camera (Gatan USC1000, USA).

Micropipette Aspiration Assay

The micropipette aspiration system consists of an inverted microscope with a 100 × oil immersed objective (IX70 Olympus, Tokyo, Japan), a micromanipulator with a resolution of ~0.2 μm (MMN-1 Narishige Co. Japan), a suction pressure unit with a resolution of 10 μm H_2O (corresponding to a minimum suction pressure of 0.98 dyn/cm^2 or 0.098 pN/μm^2), a CCD camera (WAT-902H Watec, Yamagata-Ken, Japan), and a tape recorder (Panasonic Co.).[12,23] A typical micropipette microforged to be of an inner diameter of 0.5–1.0 μm was mounted onto the micromanipulator. After zeroing the pressure at the open end, the micropipette was driven to be close to the targeted mitochondrion in solution, and a slight suction pressure was applied to trap it before suction pressure was jumped instantaneously to the preset value ranging from 25 to 150 mm H_2O (*cf.* Fig. 2f). Time course of mitochondrion deformation was recorded using a tape recorder at 25 frames per second, and the time dependence of tongue length inside the micropipette, *L*, was obtained (*cf.* Figs. 2a–e and 3a).

To conduct the mechanical measurements, 1 μL of isolated mitochondria in Dounce Buffer was injected into a customer-made chamber containing 1 mL of physiological buffer (PB) (250 mM sucrose/3 mM Hepes/0.5 mM EGTA/2 mM KH_2PO_4, pH 7.4). Membrane deformability of mitochondria was extensively tested in different physical–chemical factors of osmotic pressure and pH value, as well as in various respiratory states modulated by addition of succinate, ADP, CCCP, antimycin, Ca^{2+}, or CsA. Total 17–30 mitochondria were measured in each case. All measurements were done at room temperature (19–21 °C).

Data Analysis

Recorded images of mitochondrial deformation at a magnification of 5200× were digitalized and the dimensions were measured off-line at the resolution of ~1 pixel (~0.09 μm). At least duplicate measurements

were repeated for each dimension of micropipette diameter, intact or aspirated mitochondrion diameter or aspirated mitochondrion tongue to obtain the averaged dimension. Dimensionless tongue length (L_m/R_p) of mitochondrion was defined as the ratio of maximum length, L_m, to radius of micropipette, R_p, at the given suction pressure, ΔP. The statistical significance of (or the lack thereof) the difference between the dimensionless tongue length of mitochondrion presented in different physical–chemical and respiratory environments was assessed using the *Student t-test*.

Membrane surface tension of mitochondrion at ΔP was calculated by LaPlacian law:

$$\Delta P = 2T \times (1/R_p - 1/R_m), \quad (1)$$

where T is membrane tension and R_m is the equilibrium radius of mitochondrion. The area strain, $\Theta = \Delta A/A_0 = (A - A_0)/A_0$, where A and A_0 are the equilibrium area at ΔP and the original area at $\Delta P = 0$, respectively, was calculated using a well-known formulation,[11]

$$\Theta = \Delta A/A_0 \approx [(R_p/R_m)^2 - (R_p/R_m)^3] \times L_m/(2R_p) \quad (2)$$

The area compressibility modulus, K_{area}, of isolated mitochondria was obtained from the slope of surface tension vs. area strain fitted using a straight line.

RESULTS

Mitochondrial Morphology and Size Distribution

Isolated mitochondria from transfected T-Rex-293 cells in PB were observed as red vesicles using fluorescent microscope (Fig. 1a). In contrast to mitochondria existing in a living cell where individual mitochondrion has an elliptic geometry and tends to form the inter-mitochondrial reticulum *via* instantaneous fusions and fissions, most of mitochondria in such an *in vitro* assay presented round geometry and some of them formed small aggregates (doublets, triplets) (Fig. 1a). Ultra-microscopic observations using TEM images demonstrated that isolated mitochondria had intact inner and outer membranes (cf. Fig. 6a). Geometry of isolated mitochondria was also quantified directly from fluorescent images. As exemplified in Fig. 1b, typical size distribution had a bell shape where the peak value of mitochondrial diameter was between 0.5 to 1.5 μm. Similar size distribution of mitochondria was also found in the medium of PB/10 mM succinate, PB/10 mM succinate/0.5 mM ADP, or PB/10 mM succinate/1 mM Ca^{2+}, respectively, where the peak value also ranged from 0.5 to 1.5 μm (*data not shown*). Taken together, theses data indicated that isolated mitochondria presented stable size distribution.

Mechanical Responses of Mitochondria

A modified micropipette aspiration assay[8,12,14,23] was used to measure mechanical responses of isolated mitochondrion at a given suction pressure ΔP = 100 mm H_2O. As visualized in Figs. 2a–e, the tongue of mitochondrion went quickly into the micropipette and the mitochondrial deformation was then slowed down sharply. This was further validated by quantifying the time dependence of tongue length. As exemplified in Fig. 3a, the membrane deformation exhibited a transition phase where L increased with t and a steady phase where L reached equilibrium. The typical maximum

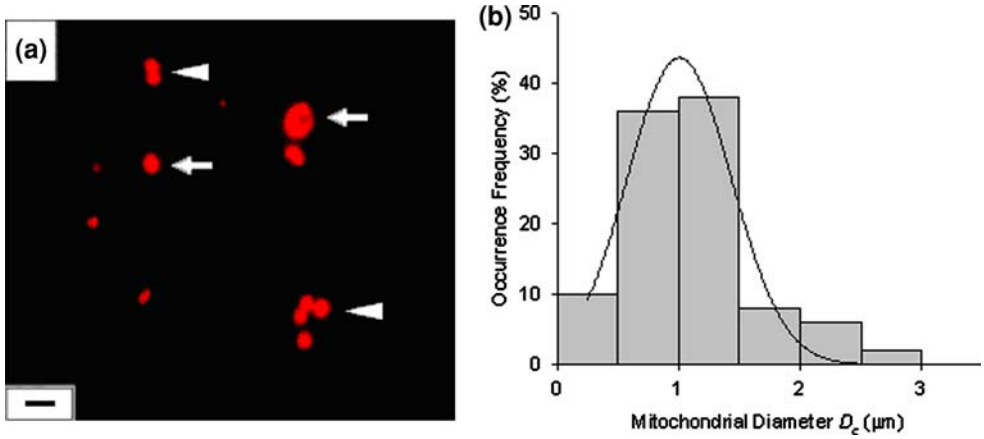

FIGURE 1. Geometry and size distribution of individual mitochondria. (a) Fluorescent images of MtDsRed labeled mitochondria isolated from transfected T-Rex-293 cells were recorded by light microscope. *Arrows* and *arrow heads* indicated single mitochondria and mitochondrial aggregates (doublets and triplets), respectively. Bar = 2 μm. (b) Typical size distribution of isolated mitochondria suspended in PB (*line* is the trend line.).

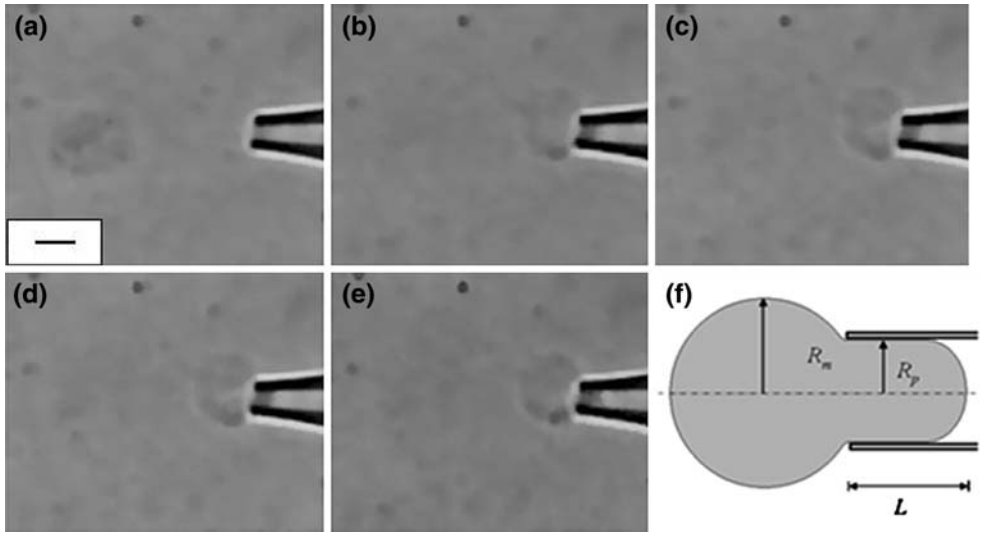

FIGURE 2. A single mitochondrion suspended in PB was aspirated at ΔP = 100 mm H_2O. Typical time course of mitochondrial deformation was presented at t = 0 (a), 120 (b), 240 (c), 360 (d), and 1200 ms (e). Bar = 2 μm. Schematic of micropipette aspiration assay was illustrated (f), where R_m and R_p are the radii of mitochondrion and micropipette, respectively, and L is aspirated tongue length.

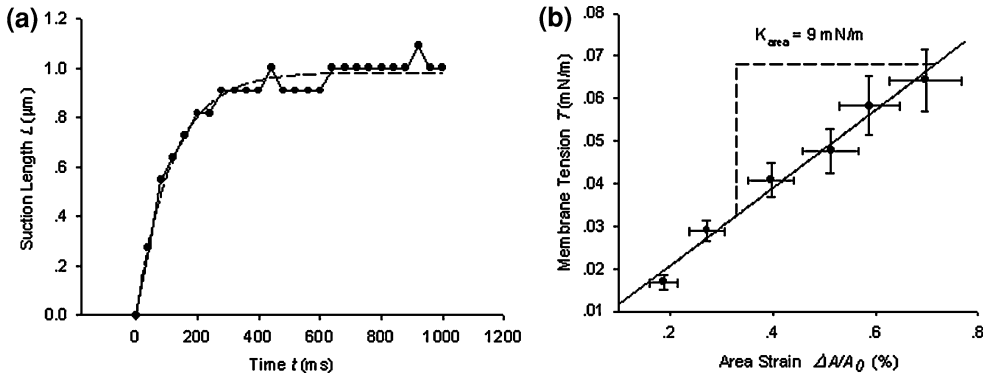

FIGURE 3. (a) Typical time dependence of aspirated tongue length of mitochondria suspended in PB at ΔP = 100 mm H_2O. *Points* are the measured data and *dash line* is the trend line. (b) Area strain dependence of surface tension for mitochondria suspended in PB at ΔP = 25–150 mm H_2O. Data (*points*) are presented as the mean ± standard errors (N = 19) (*solid line* is the linear fitted line).

tongue length, L_m, amounts to 1.09 μm where the average micropipette radius $R_p = 0.30 \pm 0.04$ μm. This turned to be the dimensionless suction length $L_m/R_p = 0.78 \pm 0.09$.

Membrane tension of isolated mitochondria was further tested by systematically varying suction pressure ranging from 25 to 150 mm H_2O (six pressures). For each mitochondrion, the equilibrium radius, R_m, where tongue length L reached L_m, was measured at the pre-set suction pressure (cf. Fig. 2f), and the aspirated mitochondrion was then released for full recovery for 5 min until another suction pressure was applied. Pre-tests of repeated aspirations at same pressure indicated that most of mitochondria were able to fully recover (*data not shown*). Membrane tension and area strain were calculated using Eqs. (1) and (2), respectively. It was found that membrane tension increased with area strain (*points* in Fig. 3b), which followed well with a simple linear fitting (*line* in Fig. 3b). The slope of fitted line represented the area compressibility modulus,[11,15] which reads to be 9 mN m^{-1}.

Effect of Osmotic Pressure and pH Value

Membrane deformability of mitochondria is significantly affected by local physical–chemical environments where mitochondria are present. To conduct the test, osmotic pressure was varied at 170, 270, and 370 mOsm in PB containing 150, 250, and 350 mM sucrose, respectively, and pH value was adjusted at 6.9, 7.4, and 7.9. Dimensionless tongue length (L_m/R_p) was used to quantify mitochondrial membrane deformability. Data indicated that the dimensionless tongue length was

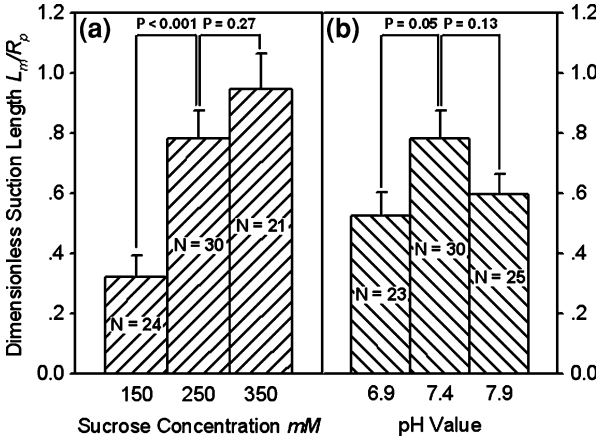

FIGURE 4. Effect of osmotic pressure and pH value on deformation of mitochondria suspended in PB. Plotted were the dimensionless suction lengths at $\Delta P = 100$ mm H_2O against the systematically varied sucrose concentrations of 150, 250, and 350 mM (a), or the systematically varied pH values of 6.9, 7.4, and 7.9 (b). Data (*bars*) were presented as the mean ± standard errors.

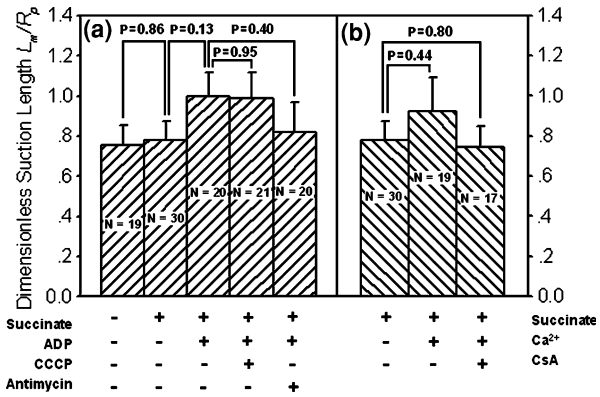

FIGURE 5. Correlation of membrane deformability with mitochondrial respiratory states or Ca^{2+} regulation. Plotted were the dimensionless suction lengths at $\Delta P = 100$ mm H_2O in PB, PB/10 mM succinate, PB/10 mM succinate/0.5 mM ADP, PB/10 mM succinate/0.5 mM ADP/2.5 μM CCCP, or PB/10 mM succinate/0.5 mM ADP/10 μM antimycin (*bars from left to right*) (a), and in PB/10 mM succinate, PB/10 mM succinate/1 mM Ca^{2+}, or PB/10 mM succinate/1 mM Ca^{2+}/10 μM CsA (*bars from left to right*) (b). Data (*bars*) were presented as the mean ± standard errors.

significantly lower at 150 mM than those at 250 and 350 mM of sucrose concentration (L_m/R_p = 0.32 ± 0.07, 0.78 ± 0.09, and 0.94 ± 0.12, respectively; $p < 0.001$ and $p < 0.001$) (Fig. 4a). This should be true since mitochondria were swollen at low osmotic pressure, which in turn stiffened the organelle. At higher sucrose concentrations of 250 and 350 mM, however, no significant differences in L_m/R_p were found (p = 0.27). By comparison, L_m/R_p was higher at pH 7.4 than those at pH 6.9 and 7.9 (0.78 ± 0.09, 0.52 ± 0.08, and 0.60 ± 0.07, respectively; p = 0.05 and p = 0.13) (Fig. 4b), suggesting that mitochondria were more deformable in the physiological pH value. It was evident that membrane deformability of mitochondria is sensitive to physical–chemical environments.

Correlation of Deformability with Respiratory Functionality

Mitochondrial functionality in cellular respiration is also correlated with their mechanical responses.[6] To test this, individual mitochondria were suspended in PB alone (State I; inactive state),[5] PB/10 mM succinate (State IV; slightly active state),[5] and PB/10 mM succinate/0.5 mM ADP (State III; active state).[5] No measurements for mitochondria suspended in PB/0.5 mM ADP (State II) were done because it is less biologically significant without the substrate.[5] Data indicated that while L_m/R_p values in States I and IV were similar (0.75 ± 0.10 and 0.78 ± 0.09, respectively; p = 0.86), they were slightly lower than that in State III (1.00 ± 0.12; P = 0.13) (*three bars from the left* in Fig. 5a), suggesting that mitochondria in active state be more deformable. It was evident that mitochondrial membrane deformability was, at least partly, correlated with their respiratory functionality. Mechanical responses of active mitochondria in State III, however, were unable to be abolished by respiratory chain inhibitors CCCP and antimycin A (1.00 ± 0.12, 0.99 ± 0.13, and 0.82 ± 0.15, respectively; p = 0.95 and p = 0.40) (*three bars from the right* in Fig. 5a).

Correlation of Deformability with Ca^{2+} Regulation

Mechanical responses of individual mitochondria are also regulated by Ca^{2+}, since Ca^{2+} is functionalized to disrupt the outer membrane and unfold the inner membrane.[1] To test this, 1 mM Ca^{2+} were added into PB/10 mM succinate. The results demonstrated that L_m/R_p was slightly lower, even without significant difference, for mitochondria suspended in the buffer without Ca^{2+} than that in the buffer supplemented with Ca^{2+} (0.78 ± 0.09 and 0.92 ± 0.17, respectively; p = 0.44) (*left and middle bars* in Fig. 5b), indicating that disruption of outer membrane and unfolding of inner membrane by addition of Ca^{2+} reduced the mechanical resistances of mitochondria. As compared to mitochondria suspended in the buffer without Ca^{2+}, L_m/R_p was maintained at the baseline level (0.74 ± 0.11; p = 0.80) when mitochondria were preincubated with immunosuppressive reagent cyclosporine A (CsA) to prevent mitochondria from Ca^{2+}-induced disruption of outer membrane and unfolding of inner membrane (*left and right bars* in Fig. 5b).

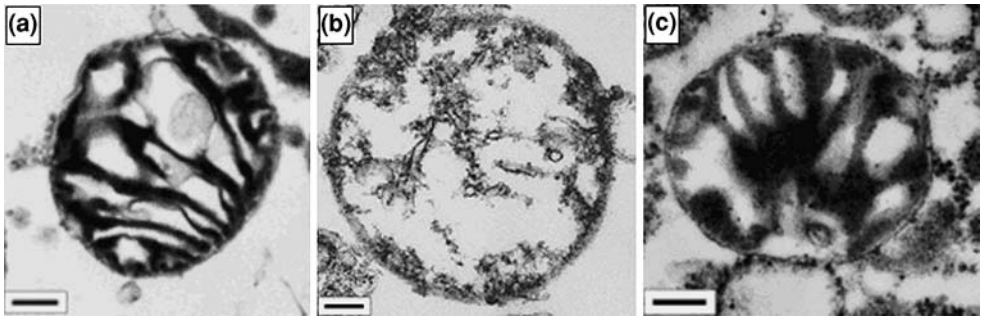

FIGURE 6. TEM images of mitochondria suspended in PB without additives (a), with the addition of 1 mM Ca^{2+} (b), or of 1 mM Ca^{2+}/10 μM CsA (c). Bar = 0.2 μm.

To further test the structural bases of the above mechanical responses, ultra-microscopic observations were performed using TEM images for mitochondria suspended in PB/10 mM succinate, PB/10 mM succinate/1 mM Ca^{2+}, and pre-incubated with CsA before adding Ca^{2+} in PB/10 mM succinate. In PB/10 mM succinate buffer, mitochondria had two intact layers of membranes without separation between the membranes, and the inner membrane was folded to form the cristae (Fig. 6a). When 1 mM Ca^{2+} were added, however, the integrity of outer membrane was broken down and the cristae were unfolded (Fig. 6b). Mitochondria were able to retain normal morphology when they were pre-incubated in CsA before adding Ca^{2+} in the buffer (Fig. 6c). Taken together, mechanical responses of individual mitochondria were apparently correlated with Ca^{2+} regulation, and the outer membrane was more mechanically resistant.

DISCUSSIONS

The goal of current work is to understand membrane deformability and membrane tension of individual mitochondria and to correlate the mechanical responses with their physiological functions. Isolated mitochondria had a bell-shaped size distribution with the most probable diameter of 1.0 μm (Fig. 1). Aspirated deformation exhibited a transition phase where the tongue length increased with time followed by a saturation phase where it reached equilibrium (Fig. 3a). This turned to be an area compressibility modulus of 9 mN m^{-1}, which was two orders-of-magnitude lower than those for red blood cells and lipid vesicles.[11,15] It should also be pointed out that the membrane tension measured here was the induced tension by suction pressure rather than the one at zero area expansion. These mechanical differences may result from various composites of surface membranes and distinctive internal structures among the vesicles.

Membrane deformability and membrane tension of mitochondria were measured by micropipette aspiration assay that has been widely used for different types of cells.[8,12,14,23] In a typical test, the time dependence of aspirated tongue length of a cell was obtained and the mechanic parameters were predicted by fitting the data to a mechanic model (e.g., a standard linear solid model).[23] Care should be taken, however, when the assay is employed for measuring the deformation of nucleated cells or complex organelles. Mitochondria have outer and inner membrane systems, and the inner membrane folds to form the cristae which ensure to accomplish their biological functions.[18] The complicated structures make it difficult to estimate directly the constitutive mechanical parameters of isolated mitochondria from a simple micropipette assay. In the current work, the maximum tongue length at a given suction pressure and the area compressibility modulus were used as apparent mechanical parameters to quantify the mechanical deformation and the surface tension of isolated mitochondria, respectively. Further investigations are required to understand the intrinsic mechanical properties of mitochondria using different mechanical models and measurements.

Membrane deformability of isolated mitochondria was affected by physical–chemical environments in buffer solution. Varying osmotic pressure or pH value in the buffer induced the changes in mitochondrial structures and functionality. For example, structural swelling and modified respiratory rates were found when the mitochondria were suspended in the buffer of non-physiological osmotic pressure.[19] Here our data indicated that lowering the osmotic pressure reduced the mitochondrial deformation, suggesting that osmotic swelling stiffened the mitochondria. Besides, the mitochondria suspended at the physiological pH value were more deformable than those at the lower or higher pH values (Fig. 4). Regardless of mechanical variations of isolated mitochondria in different osmotic pressures and pH values reported here, no significant structural

changes were found using TEM observations (*data not shown*).

Membrane deformability of isolated mitochondria was also correlated to mitochondrial respiration. Respiration is ceased when the substrate and ADP are absent (State I),[20] and slightly activated when only the substrate succinate is present (State IV).[5] This translated to the comparable deformation of isolated mitochondria. Presenting the substrate succinate and ADP induced the ADP-stimulated respiration and enhanced oxygen consumption rate (State III), which corresponded to the higher deformability. Applying CCCP (a mitochondrial uncoupler) blocked mitochondrial respiration and treatment with antimycin (an inhibitor of electron transport at complex III) caused increases in mitochondrial fragmentation, but they had no impacts on mitochondrial membrane deformability (Fig. 5a).

As an apoptotic regulator in mitochondrial physiology, Ca^{2+} induces the release of cytochrome *c* and other proteins from isolated mitochondria upon a mechanism that involves increased permeability of the inner membrane, osmotic swelling of the mitochondrial matrix, and physical disruption of the outer membrane, which is so-called the membrane permeability transition (MPT).[1,2,4,17,25] Such the Ca^{2+}-induced breakage of outer membrane and unfolding of inner membrane cristae was observed for isolated rat liver mitochondria.[1] This membrane disruption was also visualized in the current work when the substrate succinate and Ca^{2+} were presented, but was abolished when CsA (a MPT inhibitor) was pre-incubated (Figs. 6b–c). This translated to be more deformable mitochondria in the presence of Ca^{2+}. It should be pointed out, however, that mechanical responses upon Ca^{2+} regulation measured using micropipette aspiration assay were not as significantly different as expected, presumably due to limited sensitivity of mechanical measurements. Thus, more sensitive mechanical measurements may be required in further investigations to elucidate the underlying mechanism.

It should also be pointed out that the mechanical behaviors of isolated mitochondria are significantly different from those of cytoplasmic mitochondria. Inside a living cell, mitochondria tend to be elongated with multi-contoured shapes, and are embedded in the dense cytoskeletal network, suggesting that mitochondrial movement, fusion and fission are restrained physically.[13,16] Such the mechanical behaviors are also regulated by the cytoskeletal integrity and interactions between mitochondrial fusion/fission proteins and motor proteins. Even beyond the scope of the current study, our on-going works are focusing on understanding the cytoplasmic mitochondrial movement, fusion, and fission regulated by disrupting the cytoskeleton network, and by blocking the physical linkage between cytoskeletal proteins and motor proteins.

Finally, our results indicated that mitochondrial membrane deformation was regulated by physical–chemical environments in the buffer, and were correlated with their respiratory functions. These results provided a new insight into biomechanical bases for mechanical regulation of mitochondrial functionality.

ACKNOWLEDGMENTS

We are grateful to Center of Electron Microscopy, Institute of Biophysics, Chinese Academy of Sciences to provide TEM device, and to Lei Sun for TEM sample preparation, observation and useful discussions. This work was supported by National Natural Science Foundation of China grants 10332060 and 30730032, National Key Basic Research Foundation of China grant 2006CB910303, and Chinese Academy of Sciences grant 2005-1-16 (M.L.).

REFERENCES

[1]Andreyev, A., and G. Fiskum. Calcium induced release of mitochondrial cytochrome *c* by different mechanisms selective for brain *versus* liver. *Cell Death Differ*. 6:825–832, 1999.

[2]Armstrong, J. S. Mitochondrial membrane permeabilization. The *sine qua non* for cell death. *Bioessays* 28:253–260, 2006.

[3]Bandyopadhyay, S. K., and A. Dutta. Mitochondrial hepatopathies. *J. Assoc. Physicians India* 53:973–978, 2005.

[4]Brustovetsky, N., T. Brustovetsky, R. Jemmerson, and J. M. Dubinsky. Calcium-induced cytochrome *c* release from CNS mitochondria is associated with the permeability transition and rupture of the outer membrane. *J. Neurochem*. 80:207–218, 2002.

[5]Chance, B., and G. R. Williams. Respiratory enzymes in oxidative phosphorylation III the steady state. *J. Biol. Chem*. 217:409–427, 1955.

[6]Chvanov, M. Metabolic control of elastic properties of the inner mitochondrial membrane. *J. Phys. Chem. B* 110:22903–22909, 2006.

[7]Darin, N., G. Kollberg, A.-R. Moslemi, M. Tulinius E. Holme, M. A. Grönlund, S. Andersson, and A. Oldfors. Mitochondrial myopathy with exercise intolerance and retinal dystrophy in a sporadic patient with a G583A mutation in the mt tRNA(phe) gene. *Neuromuscul. Disord*. 16:504–506, 2006.

[8]Evans, E., and A. Yeung. Apparent viscosity and cortical tension of blood granulocytes determined by micropipet aspiration. *Biophys. J*. 56:151–160, 1989.

[9]Feiguin, F., A. Ferreira, K. S. Kosik, and A. Caceres. Kinesin-mediated organelle translocation revealed by specific cellular manipulations. *J. Cell Biol*. 127:1021–1039, 1994.

[10]Galluzzi, L., N. Larochette, N. Zamzami, and G. Kroemer. Mitochondria as therapeutic targets for cancer chemotherapy. *Oncogene* 25:4812–4830, 2006.
[11]Kwok, R., and E. Evans. Thermoelasticity of large lecithin bilayer vesicles. *Biophys. J*. 35:637–652, 1981.
[12]Long, M., Z. Wu, H. Wang, G. Song, X. Wang, and Y. Wu. Experimental investigation on viscoelasticity of hepatocytes. *Acta Bioph. Sin*. 12:169–173, 1996.
[13]Miller, K. E., and M. P. Sheetz. Axonal mitochondrial transport and potential are correlated. *J. Cell Sci*. 117:2791–2804, 2004.
[14]Needham, D., and R. M. Hochmuth. A sensitive measure of surface stress in the resting neutrophil. *Biophys. J*. 61:1664–1670, 1992.
[15]Nichols-Smith, S., S. The, and T. L. Kuhl. Thermodynamic and mechanical properties of model mitochondrial membranes. *Biochim. Biophys. Acta*. 1663:82–88, 2004.
[16]Penman, S. Rethinking cell structure. *Proc. Natl. Acad. Sci. USA* 92:5251–5257, 1995.
[17]Petit, P. X., M. Goubern, P. Diolez, S. A. Susin, N. Zamzami, and G. Kroemer. Disruption of the outer mitochondrial membrane as a result of large amplitude swelling: the impact of irreversible permeability transition. *FEBS Lett*. 426:111–116, 1998.
[18]Scheffler, I. E. Mitochondria make a come back. *Adv. Drug Deliv. Rev*. 49:3–26, 2001.
[19]Sitaramam, V., D. Sambasivarao, and J. C. Mathai. Differential effects of osmotic pressure on mitochondrial respiratory chain and indices of oxidative phosphorylation. *Biochim. Biophys. Acta*. 975:252–266, 1989.
[20]Toleikis, A., S. Trumbeckaite, and D. Majiene. Cytochrome *c* effect on respiration of heart mitochondria: influence of various factors. *Biosci. Rep*. 25:387–397, 2005.
[21]Varadi, A., L. I. Johnson-Cadwell, V. Cirulli, Y. Yoon V. J. Allan, and G. A. Rutter. Cytoplasmic dynein regulates the subcellular distribution of mitochondria by controlling the recruitment of the fission factor dynamin-related protein-1. *J. Cell Sci*. 117:4389–4400, 2004.
[22]Wagner, O. I., J. Lifshitz, P. A. Janmey, M. Linden, T. K. McIntosh, and J.-F. Leterrier. Mechanisms of mitochondria-neurofilament interactions. *J. Neurosci*. 23:9046–9058, 2003.
[23]Wu, Z., G. Zhang, M. Long, H. Wang, G. Song, and S. Cai. Comparison of the viscoelastic properties of normal hepatocytes and hepatocellular carcinoma cells under cytoskeletal perturbation. *Biorheology* 37:279–290, 2000.
[24]Yaffe, M. P. The machinery of mitochondrial inheritance and behavior. *Science* 283:1493–1497, 1999.
[25]Yi, M., D. Weaver, and G. Hajnóczky. Control of mitochondrial motility and distribution by the calcium signal: a homeostatic circuit. *J. Cell Biol*. 167:661–672, 2004.